AIR-SEA CARBON DIOXIDE FLUXES IN THE COASTAL ZONE

Lucía Gutiérrez Loza and Francisco J. Ocampo-Torres

Physical Oceanography Department, CICESE, Carretera Ensenada-Tijuana 3918, Ensenada, BC 22860 (México),
Email: lugutier@cicese.edu.mx

ABSTRACT

Gas exchange processes between ocean and atmosphere are commonly parametrized as a wind speed function. However, in coastal waters many physical processes occur due to the presence of ocean surface waves, having an important influence on the air-sea interaction and gas flux behavior.

Time series of significant wave height, CO_2 and H_2O fluxes from May 15 to September 11 of 2014, were analysed so the effect of ocean surface waves on the flux behavior could be assessed to some point.

1. INTRODUCTION

The CO_2 gas exchange between ocean and atmosphere is one of the most important processes involved in the global carbon cycle [8]. Hence, the understanding of the mechanisms that control the gas exchange is of great importance and could lead us to improve our knowledge on the global carbon inventory and reduce uncertainties in global climate models.

The gas exchange through the ocean surface occurs by diffusivity due to the difference in the gas concentration between air and water phases, but the efficiency of transfer processes is also important. Such efficiency is related to the turbulence that modifies the behavior of the diffusive layer, and may be represented as a flux resistance by the surface and expressed as a function of the transfer velocity (k) [5].

Usually, k is parametrized as a wind speed function but there are many other processes involved in the gas transfer that should be considered. [1],[5],[8] and [9] have presented functions including multiple parameters , even so, in coastal waters many physical processes occur due to the presence of ocean surface waves and its influence on the air-sea interaction and flux behavior must be validated.

2. METHODS

2.1 Study Site

Direct measurements of CO_2 fluxes (FCO_2) and water vapor fluxes (FH_2O) were carried out in a coastal station at Punta Morro (PM), located at 31°51'411N, 116°40'07''W, in the Northwest of Todos Santos Bay (TSB), Baja California, México (Fig. 1).

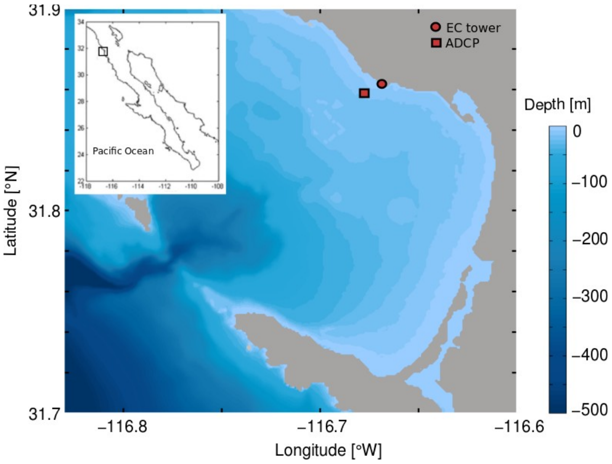

Figure 1. Map of the site at PM in the Northwest of TSB showing the location of the EC tower (red circle) and the ADCP (red square).

The eddy covariance (EC) tower is located right in the shoreline and implemented with an infrared open-path gas analyzer (LI-7500, LICOR, Lincoln, NE, USA) and a sonic anemometer (R3-100 Professional 3D Anemometer, Gill Instruments, Lymington, Hampshire, UK), both at a height of 13m above the mean sea level and with sampling rate of 20Hz.

A cleaning system was installed in the infrared gas analyzer to improve its performance by decreasing the optical contamination. The system was implemented with a small pump that delivers three jets of isopropyl alcohol every four hours into the top and bottom optical windows to remove salt contamination. This allowed us to have lower Automatic Gain Control (AGC) values than cases without the cleaning system.

2.2 Flux Estimation

The EC method has become the primary method used for gas flux estimation in terrestrial studies but also used in coastal and open ocean environments [4]. Through this method it is possible to directly estimate gas fluxes with a high temporal resolution using the correlation of the turbulent fluctuations of the vertical wind speed and the gas concentration. The general EC equation is:

$$FCO_2 = \overline{\rho_a w' s'} \qquad (1)$$

Where ρ_a is the mean air density, w is the vertical wind speed and s is the mixing ratio. The primes indicates that these values are the turbulent fluctuations and the overbar indicates the time average.

In this study, the FCO_2 and FH_2O were estimate through EC method considering a 15 minutes average period selected based on a cumulative cospectrum analysis. Only on-shore wind directions (135°-315°) were taken into account.

2.3 Waves information

For the same measurement period (May 15 to September 11, 2014) hourly information of waves were recorded at 2Hz using an Acustic Doppler Current Profiler (Workhorse Sentinel, Teledyne RD Instruments, Poway, CA, USA) at a depth of 10m in a site 400m away form the tower.

3. RESULTS

Low to moderate wind speed conditions (~4m/s), mainly from the Northwest, prevailed during the study with a highest value of 11.5m/s (Fig. 2A). Maximum significant wave height (H_s) recorded was 1.23 and the predominant incoming wave direction was found to be from Southwest as shown in Fig. 2B, this occur due to refraction of the waves inside TSB.

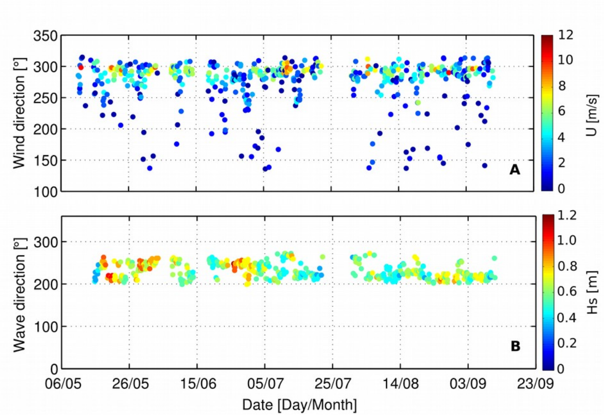

Figure 2. Time series of (A) incoming wind direction and (B) incoming waves direction. In the top panel color represents the magnitude of the wind speed, in the bottom panel color represents H_s.

From data shown in Fig. 3A, we found PM to be a sink of CO_2 from May to September with a mean FCO_2 and standar deviation of -2.4±4.5μmol/m^{2}s; Values of FCO_2 are in accordance with previous results obtained by [4] nearby at Todos Santos Island. The mean value and standard deviation found for FH_2O were 0.6±2.8mmol/m^{2}s (Fig. 3B).

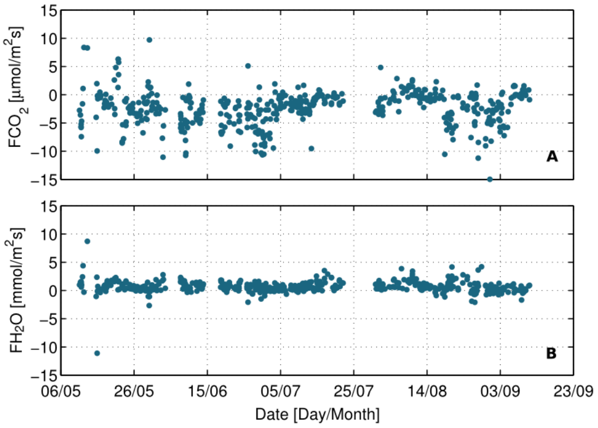

Figure 3. Time series of (A) FCO_2 and (B) FH_2O for each 15 minutes average period.

The relation between wind speed and both, FCO_2 and FH_2O exist (Fig. 4). However, the correlation coefficient (r) values of -0.39 and 0.43, respectively, indicate that the correlation is not as large as could be expected given that most of the parametrizations for flux estimation are function of the wind speed. At least for the conditions encountered in this study of coastal waters, the influence of other physical processes besides wind is confirmed.

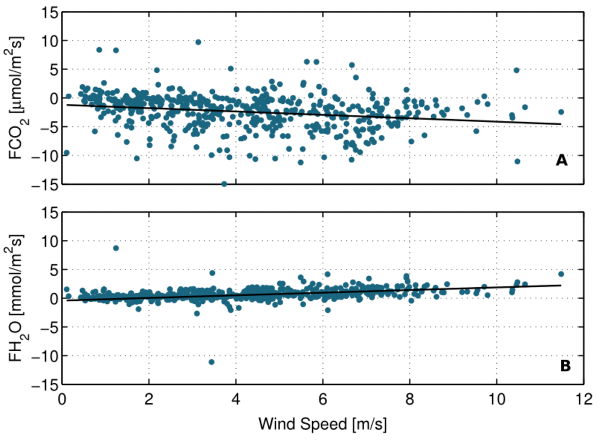

Figure 4. (A) FCO_2 and (B) FH_2O vs. wind speed. The solid line is the linear regression that fits the data.

On the other hand, the dependency of FCO_2 with H_s, shown in Fig. 5A, has an r value of -0.42. This relation does not exist for FH_2O (Fig. 5B).

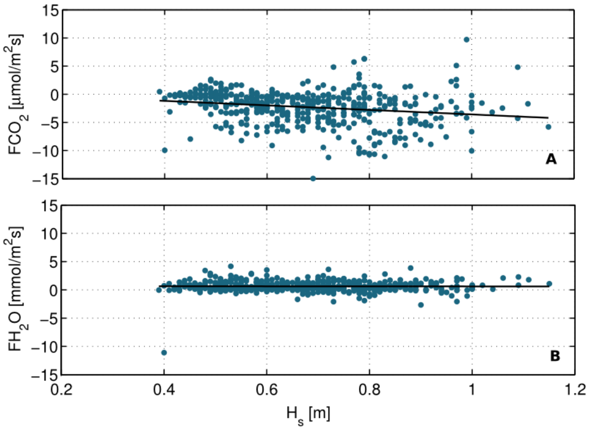

Figure 5. (A) FCO_2 and (B) FH_2O vs. H_s. The solid line is the linear regression that fits the data.

The highest correlation (r=-0.45) was found between FCO_2 and the wave steepness. The later one obtained from the ratio of H_s and the mean absolute wave length (L_m), being indicative of wave stability, and hence, of the wave breaking.

Even when data shown in Fig. 6 is not representative of the wave breaking in the coast, it can be thought that there will be an increase in FCO_2 as the wave steep increases when approaching the coast, further analysis will be made in this regard. This assumption is comparable with the breaking-wave hypothesis proposed by [7], where they attribute the increase in FCO_2 to the turbulence associated with the breaking waves.

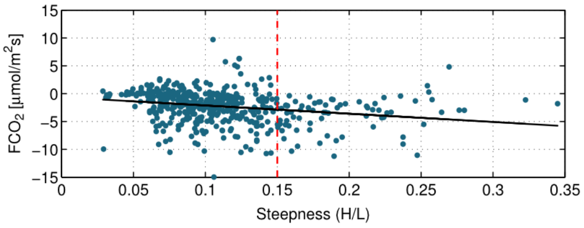

Figure 6. FCO_2 vs. wave steepness. The red dashed line is the theoretical threshold for wave stability.

4. CONCLUSIONS

We found the study area to be a sink of CO_2 in the period from May to September under low to moderate wind and wave conditions (mean FCO_2=-2.4μmol/m^{2}s). The highest correlation was found to be between FCO_2 and wave steepness with an r=-0.45.

Further analysis of the data is needed to achieve a quantitative evaluation of the effect of ocean surface waves on gas exchange in the coastal zone. However, these results show a tendency of increasing FCO_2 to the ocean with the significant wave height, and even more, with the increase of wave steepness.

The behavior of the FH_2O is less correlated to wind and waves conditions than FCO_2, as expected, because the resistance to transfer resides in the gas phase rather than in the aqueous phase where the turbulent processes associated with the sea state are being evaluated.

Based on the AGC values (not shown) retrived, we can assure that the cleaning system used in the infrared gas analyzer is an essencial feature to guarantee the good quality of the data.

Acknowledgements. *This study is part of the "Sea Surface Roughness as Air-Sea Interaction Control" (RugDiSmarCTRLo-a) CONACyT proyect (155793). We thank CICESE's Physical Oceanography Department, the European Geoscience Union (EGU) and the European Space Agency (ESA) for their financial support. To J. Martínez, R. Alcaráz, E. Rivera, V. Toro and G. García for the technical help related to the experimental set-up and maintenance. Finally, to P. Osuna for his advices and support, and to the rest of the CICESE's waves group for their contributions to this work.*

5. REFERENCES

1. Mörk, E., Sorensen, L., Jensen, B. & Sejr, M. (2014). Air-sea CO_2 gas transfer velocity in a shallow estuary. *Boundary-Layer Meterology*, **151**, 119-138.

2. Norman, M., Rutgersson, A., Sørensen, L. & Sahlée, E. (2012). Methods for estimating air–sea fluxes of CO_2 using high-frequency measurements. *Boundary-Layer Meteorology*, **144**, 379-400.

3. Ocampo Torres, F. J. & García Nava, H. (2007). La interacción entre el océano y la atmósfera: aspectos físicos relevantes en la transferencia de gases. In "Carbono en ecosistemas acuáticos de México" (Eds. B. Hernández de la Torre & G. Gaxiola Castro), Instituto Nacional de Ecología, México, p. 29-42.

4. Reimer, J., Vargas, R., Smith, S., Lara-Lara, R., Gaxiola-Castro, G., Hernández-Ayón, J., Martínez-Osuna, J. (2013). Air-sea CO_2 fluxes in the near-

shore and intertidal zones Influenced by the California Current. *Journal of Geophysical Research*, **118**, 1-16.

5. Rutgersson, A. & Smedman, A. (2010). Enhanced air–sea CO_2 transfer due to water-side convection. *Journal of Marine Systems*, **80**, 125-134.

6. Rutgersson, A., Smedman, A. & Sahlée, E. (2011). Oceanic convective mixing and the impact on air-sea gas transfer velocity. *Geophysical Research Letters*, **38**(L02602).

7. Smith, S. & Jones, E. (1985). Evidence for wind-pumping of air-sea gas exchange based on direct measurements of CO_2 Fluxes. *Journal of Geophysical Research*, **90**, 869-875.

8. Suzuki, N., Donelan, M., Komori, S. & Takagaki, N. (n.d.). Estimation of the global air-sea CO_2 gas flux considering wave breaking. *Journal of Oceanography*, (In review).

9. Zhao, D., Toba, Y., Suzuki, Y., & Komori, S. (2003). Effect of wind waves on air-sea gas exchange: Proposal of an overall CO_2 transfer velocity formula as a function of breaking-wave parameter. *Tellus B*, **55**(0280-6509), 478-487.